Granular Material Flows with Interstitial Fluid Effects
NAG3-2358
Final Report
Melany L. Hunt and Christopher E. Brennen

The research focused on experimental measurements of the rheological properties of liquid-solid and granular flows. In these flows, the viscous effects of the interstitial fluid, the inertia of the fluid and particles, and the collisional interactions of the particles may all contribute to the flow mechanics. These multiphase flows include industrial problems such as coal slurry pipelines, hydraulic fracturing processes, fluidized beds, mining and milling operation, abrasive water jet machining, and polishing and surface erosion technologies. In addition, there are a wide range of geophysical flows such as debris flows, landslides and sediment transport. In extraterrestrial applications, the study of transport of particulate materials is fundamental to the mining and processing of lunar and Martian soils and the transport of atmospheric dust (National Research Council 2000). The recent images from Mars Global Surveyor spacecraft dramatically depict the complex sand and dust flows on Mars, including dune formation and dust avalanches on the slip-face of dune surfaces. These Aeolian features involve a complex interaction of the prevailing winds and deposition or erosion of the sediment layer; these features make a good test bed for the verification of global circulation models of the Martian atmosophere.

When we initiated our research, we argued that in many particle-flow applications the rheological properties are based on the classic liquid-solid suspension studies by Bagnold from the 1950's (Bagnold 1954). In his seminal experiments, 1-mm wax spheres suspended in a glycerin-water-alcohol mixture were sheared in an annular coaxial rheometer. The rheometer was designed to measure both the shear and normal forces applied to the walls. From his measurements and analysis, Bagnold identified two regimes of flow. For small shear rates, in viscous liquids the shear stresses were found to behave like a Newtonian fluid with a corrected viscosity; in addition, normal forces were also generated. In this "macroviscous" regime, both the normal and the tangential stresses were linearly proportional to the liquid's dynamic viscosity (μ), the shear rate (γ) and a function of the solid concentration, $\lambda^{3/2}$ where λ depends on the solid fraction (ϕ). Bagnold proposed that the normal stresses were generated by the viscous resistance of the fluid as it was squeezed between sheared particles. For larger shear rates or for lower liquid viscosities, the material fell into the "grain-inertia regime" in which the stresses were independent of the fluid viscosity and depended on the square of the shear rate, the square of the particle diameter (d), the particle density (ρ_p) and showed a stronger dependence on the solids concentration, λ^2. Bagnold also suggested a distinction between the two regimes by defining a parameter from the ratio of the scalings for the stress, N where $N = \rho_p d^2 \gamma^2 \lambda^2 / \lambda\gamma\lambda^{3/2} = \rho_p d^2 \lambda^{1/2} \gamma / \mu$ (often referred to as the Bagnold number). Note that the particle density equaled the fluid density in Bagnold's experiment.

Although this work has been cited hundreds of times in the literature, the experimental results have never been verified by an independent set of experiments. In addition, the original work was limited to neutrally-buoyant single-sized particles, but the rheological properties have been extended to a range of applications in which the particles

were denser than the fluid, including work on magma flows, debris flows, Aeolian transport and granular material flows. In our original proposal, we outlined a series of experiments that could be done to expand the rheological database by including experiments in which the particle phase was denser than the fluid phase and in which the particles would not sediment.

In preparing for our experiments, we did a careful examination of Bagnold's data. Through this analysis, we demonstrated that Bagnold's experiments had significant secondary flow effects because the height (h) of the rheometer was relatively short compared to the spacing (b) between the rotating outer and stationary inner cylinders (h/b=4.6). Since the top and bottom end plates rotated with the outer cylinder, the flow contained two axisymmetric counter-rotating cells in which flow moved outward along the end plates and inward through the midsection of the annulus. To account for the secondary flows, we performed finite element simulations of the flow within the annulus for Bagnold's flow conditions. At rotational speeds beyond a critical value, these cells contributed significantly to the measured torque. We showed that Bagnold's suspension measurements could be explained assuming laminar Newtonian flow and using a corrected viscosity that depends on the solids concentration. Hence, the effect of the particles was to increase the viscosity of the fluid and decrease the flow Reynolds number (based on the rotational speed of the outer wall and the gap spacing). For the highest Reynolds number in Bagnold's experiments, the flow may have transitioned to turbulent flow. The normal stress measurements were difficult to predict because of the experimental design but appear to be related to the centrifugal forces. As a result, collisional interactions between particles were probably not present in Bagnold's experiment. In addition, it now appears that there is no appropriate rheological data to use in a wide class of problems involving liquid-solid flow.

The focus of our experiments has been to measure the shear and normal forces in a shear flow containing solid particles in a liquid. These experiments will provide a unique opportunity for exploring the transition from transport in a pure Newtonian fluid to transport occurring during a dense flow of particles. By carrying out the experiments in reduced gravity we will be able to use fluids and particles of differing densities without encountering problems associated with sedimentation or flotation. The experimental database resulting from our measurements will show the dependence of the stresses on the Stokes and Reynolds number, concentration, and other experimental parameters (such as the stiffness of the particles, gap size relative to particle diameter, and density ratio). The experiments will be operated for Stokes and Reynolds numbers in which the inertial contributions of both phases will be important. These results will also allow us to develop constitutive models for these flows.

A cut-away drawing of the experimental facility is shown in Fig. 1. The rheometer consists of two co-axial stainless steel drums. The particles plus fluid are contained within the annular region. The outer drum is rotated at speeds up to 400 rpm using a friction belt drive system driven by a 2-hp three-phase motor mounted on the frame. The inner drum is held stationary supported at each end on a framework of extruded aluminum sections. There are roller bearings at each end along with a spring-energized lip seal mounted on the wet side of the bearings. The radius of the inner cylinder is 0.159 m (6.25 in) and the gap width (b) is 0.0316 m (1.25 in). The overall height of the annulus (h)

is 0.369 m (14.5 in). The entire assembly is made from 304 stainless steel to prevent corrosion.

The inner cylinder consists of a top and bottom guard cylinder and an instrumented test cylinder. The test drum is 0.112 m (4.42 in) in height and each of the guard cylinders are 0.127 m (5 in). The test cylinder is a thin-walled drum with each edge machined to a knife-edge finish to minimize the chances of particles becoming caught between the test drum and the adjoining guard sections. By using the guard cylinders, the torque on the test cylinder can be measured directly and the effects associated with the fluid rotation in the ends of the annulus can be minimized. Note that the top and bottom endplates do not rotate. Although the ratio of the total annulus height to gap (h/b=11.6) is limited, the stationary end pieces decrease the secondary flow effects. We have also carried out finite element simulations of our facility and have been able to demonstrate the differences between the rotating and stationary end plates.

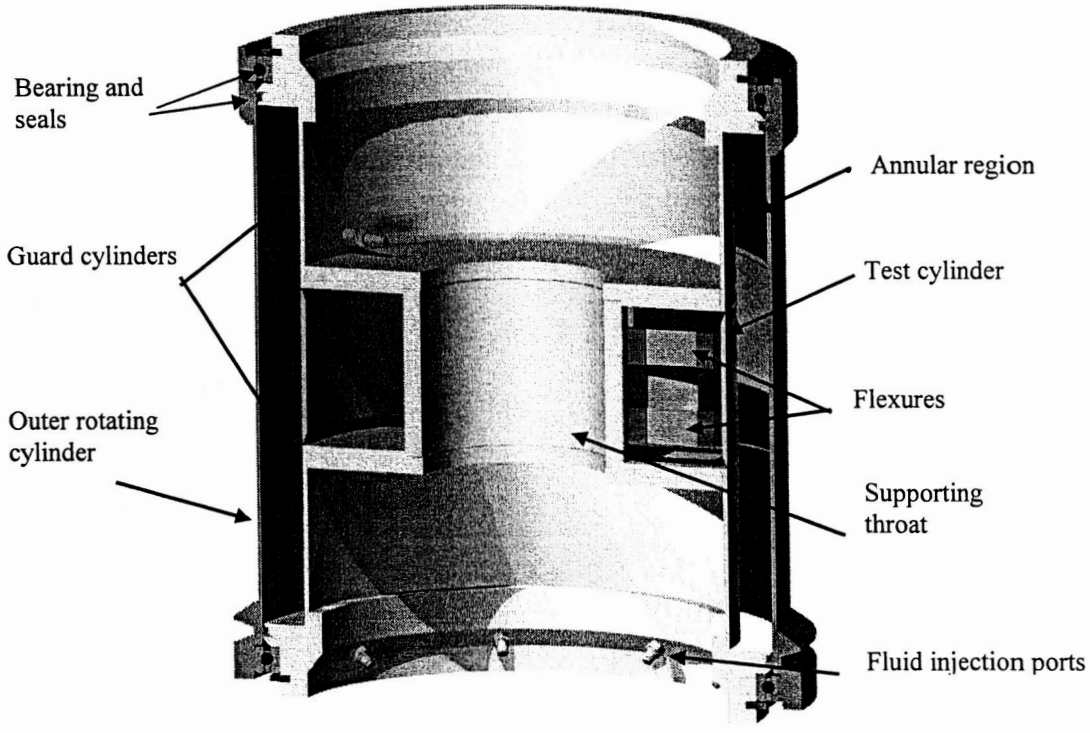

Figure 1. Cut away drawing of the assembled experimental apparatus showing the annular region, the flexures, the inner throat section, fluid injection ports, bearings and seals. The two plugs on the upper and lower guard cylinders are the piezoelectric transducers for the particle pressure measurements.

The test drum is mounted onto the inner throat using a system of flexures and brackets as shown in the picture and sketch of Fig. 2. The flexures are thin sections of stainless steel that connect the test drum to the throat. As shown in the figure, two flexures are used at each of three circumferential positions to give the flexures rigidity in the axial direction. The flexures support the test drum and allow it to rotate slightly when

a load is applied tangentially to the test drum. From the deflection, we can determine the torque applied to the cylinder and thus the shear force resulting from the fluid motion within the gap. The deflection is measured using a temperature-compensated MicroStrain Non-Contact Differential Variable Reluctance Transducers (NCDVRT) paired with a magnetic target (1 cm diameter disc of 410 stainless steel – a magnetic material); the sensor-target pairs are located at each of the 3 flexures positions. The transducer consists of a stainless steel threaded cylinder (1.27 cm diameter) that contains a sense coil and a temperature compensation coil. When a ferrous or highly conductive object is moved in close proximity to the sensing face the magnetic reluctance of the circuit formed between the sense coil and the object changes. Hence, the signal from the reluctance transducers decreases as the flexures are torqued. The targets are mounted on a small Delrin plate so it can be micro-adjusted to allow for zero calibration of the sensors. Both the targets and sensors are mounted from the throat. The flexures can be changed to provide a range of stiffness and thickness, and hence a large range of measurable torques. The system is also designed with stops to prevent the test cylinder from over rotating.

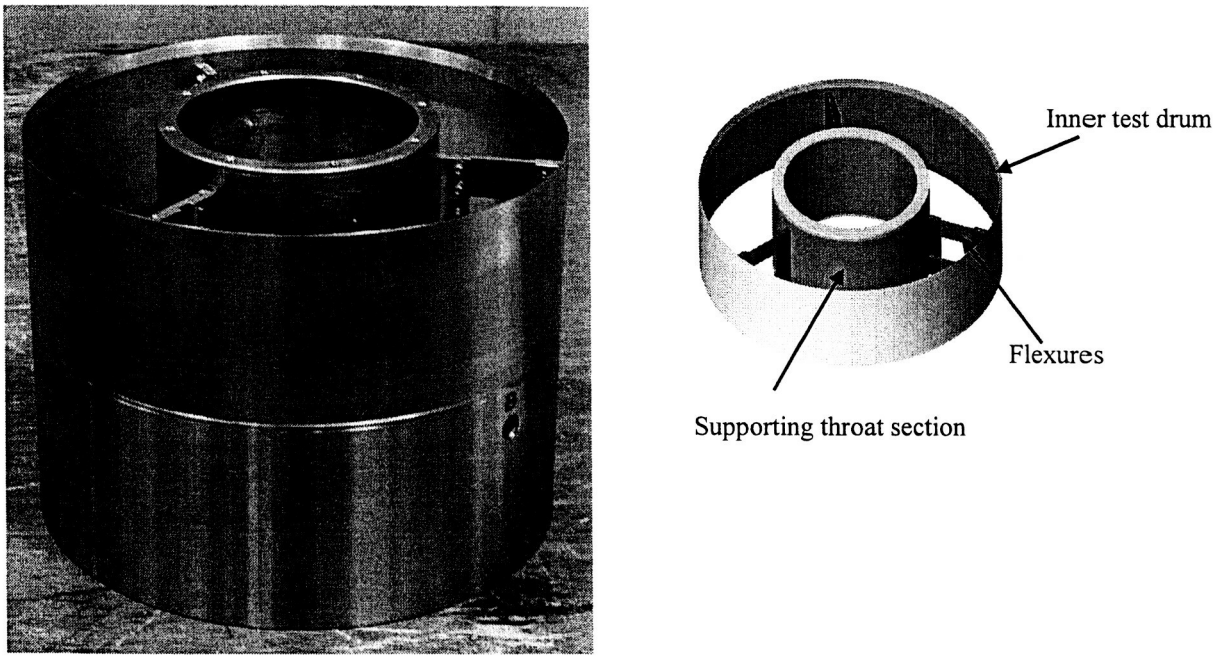

Fig. 2.The picture and sketch show the inner test drum, 6 flexures with mounting brackets at 3 different circumferential locations, and the supporting throat section. The picture also shows the lower guard cylinder with the port marked "B" for the piezoelectric transducers. The variable reluctance displacement transducers are not shown.

The fluid-particle flow within the annulus also produces a normal collisional stress. This stress is measured using a technique that we developed in earlier studies using high-frequency-response (1 μsec rise time) piezoelectric pressure transducers. The normal pressure is obtained by measuring the collision impulses over an extended period of time. The experimental facility includes two piezoelectric transducers: one mounted on the

upper guard cylinder and the second on the lower guard cylinder. Both transducers are located 2 cm from the test drum, as indicated in Fig. 1. From these transducers, we can also record the collision frequency. Hence, we will be able to determine if the collision rate is approximately constant across the test cylinder.

The rheometer is also equipped with a fluid recirculation system including 8 fluidization jets on the lower flange of the annulus, as shown in Fig. 1. These injection jets are included to help distribute and mix the particles. Fluid is returned through a port in the region between the test drum and the inner throat. When the experiment is flown in the low-gravity plane, the particles will settle during the high gravity period. The fluidization will help disperse the particles within the annulus prior to the low-gravity portion of the flight. Hence, the fluidization will only be used when needed during parabolic flights. The system, however, also provides a means for changing fluids. Through the pumping system, we are able to add a glycerin/water mixture to change the fluid viscosity. The knife-edge seal between the test drum and the guard drums will prevent solids from entering the circulation loop. In addition a 20-micron inline filter will extract fine impurities from the fluid as it is circulated. The fluid injection jets are sized to prevent contamination by solids. To allow for the thermal expansion of the liquid during flight a sealed expansion tank is incorporated into the circulation loop.

We have also designed and built a small sight-glass with a single jet, which can be used to inspect visually the fluidization process both on the ground and during flight. The sight glass is made from a Lucite tube with a sealed bottom flange; the upper piece is sealed with a gasket. It will be filled with the same fluid and particle concentration as contained in the rheometer. We can also use the watch glass to determine whether the particles are free floating and when they are settled under gravity. It also contains a single injection and withdrawal port that can be connected to the fluid circulation unit to test the fluidization process. The volume of the sight glass is approximately equal to one-eighth the volume of the rheometer; hence the single injection port will displace an approximately equivalent amount of particles as found in the rheometer. The sight-glass can be mounted vertically as part of the external structure of the experiment.

Figure 3 shows the current experiment with the supporting structure, the motor, the fluidization pump as it is being used in the laboratory. The large fluidization pump is replaced by a smaller unit for flight experiments. For the flight experiments, Lexan sheets are used to enclose the facility.

We have extensively tested the torque measurements on the inner drum using the variable reluctance transducers. The output signal varies non-linearly with displacement between –5 and +5 Volts DC for the full range of the sensor (approximately 3 mm maximum displacement). This displacement is related to torque using a calibration that is acquired for each experimental setup. We have been able to obtain consistent measurements of torque in the range from 0.04 to 30 Nm, which is accomplished by changing the flexures. To date, we have tested 5 different flexures ranging from 0.1 to 0.635 mm (0.004-0.025 in). For a flexure thickness of 0.1 mm at a maximum displacement of 2 mm, we measured a torque of 0.048 Nm with a resolution of one percent. As a result, we should be able to make torque measurements over a wide range of rotational speeds, particle concentrations, and fluid viscosities. These calibration

experiments have been performed in air and in water-plus-glycerin with no difference in the performance of the transducer.

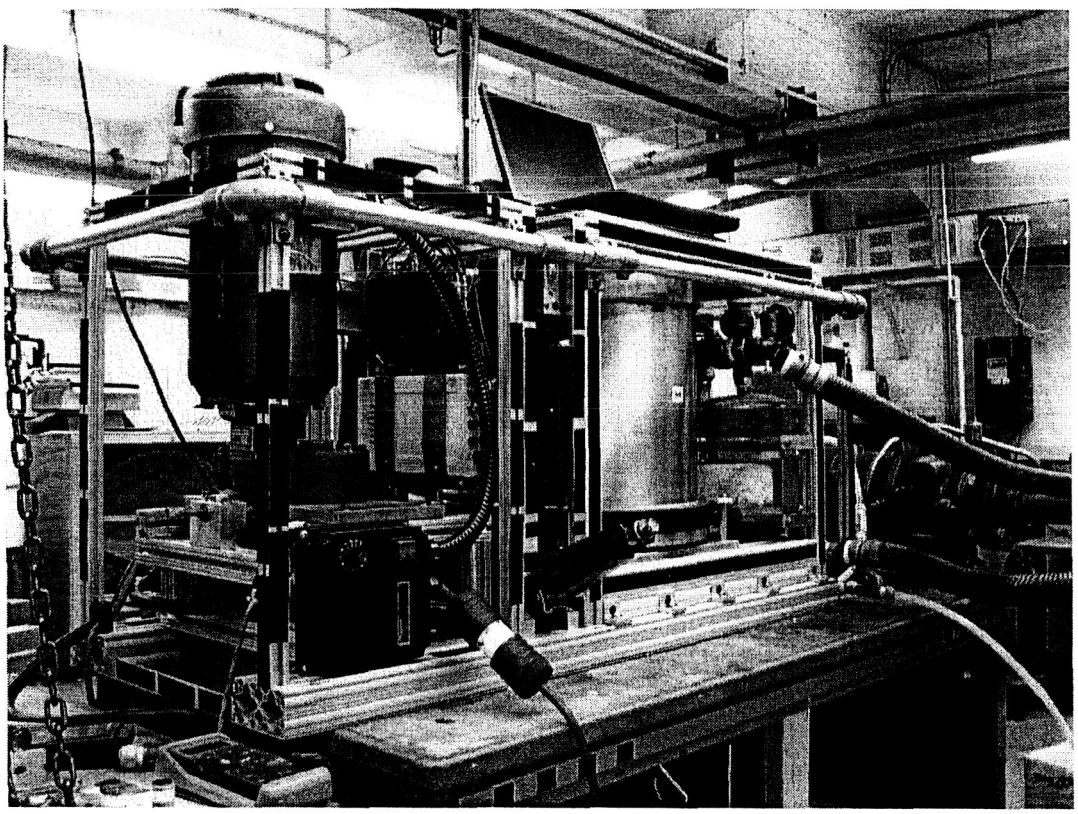

Figure 3. Experimental apparatus as used in the laboratory.

The normal stress measurements have been tested using a simple particle pendulum, as done in our earlier experimental work. The particle is released from rest and directed at the transducer. The trajectory of the particle is recorded using a high-speed imaging system to determine the particle speed at impact. As the particle impacts the transducer, the pressure as a function of time is recorded. This signal is integrated over time to determine the pressure impulse. For high Stokes numbers (such as in dry flows), the pressure impulse increases linearly with the mass of the particle and the impact speed; these results can be directly compared with the manufacturer's calibration of the transducer. At lower Stokes numbers, the measured pressure impulse decreases due to lubrication effects. We find that the pressure signal can be adequately resolved for Stokes numbers greater than about 10. For lower Stokes numbers, it is difficult to distinguish the normal collisions from background noise.

Measurements are acquired from sensors on the test rig using a data-acquisition system built into a laptop personal computer. We are using two different data acquisition cards – one high-speed card for the piezoelectric transducers and a second card for the other transducers including the displacement sensors. We also have a magnetic pickup on the motor for the speed and will use the on-board accelerometer for the flight

experiments. A thermistor is also installed in the region behind the test cylinder to monitor the temperature of the fluid.

One series of low-gravity flight experiments were conducted experiments for glass beads in water and water-glycerin mixtures. These experiments indicated that there was a tremendous need to increase the fluidization capability of the facility. The facility has been modified in recent months to remedy the problems. We are currently scheduled for a second round of flights during May, 2004. In addition, we have been doing ground based measurements using lighter particles and the fluidization system to maintain a distribution of particles.

Publications

Hunt, M.L., Zenit, R., Campbell C.S. & Brennen, C.E. (2002) Revisiting the 1954 suspension experiments of R.A. Bagnold, ***J. Fluid Mechanic,* 452,** 1-24.

A.V. Potapov, M.L. Hunt & C.S. Campbell, (2001) Liquid-solid flows using smoothed particle hydrodynamics and the discrete element method, Powder Technology, 16, 204-213.